The Radiopharmaceutical Chemistry of Metallic Radionuclides

6

Aohan Hu and Justin J. Wilson

6.1 The Fundamentals: Overview of the Chemical Properties of Metal Ions

A wide variety of radioisotopes of metallic elements—or radiometals—could be harnessed for radiopharmaceutical therapy (RPT) (Table 6.1) based on their favorable physical decay properties [1–3]. The successful implementation of these radiometals in therapeutic nuclear medicine requires an extensive understanding of their chemical properties. As shown in Table 6.1, these radiometals span nearly the entire periodic table, with key candidates within the main-group elements, transition metals, lanthanides, and actinides. As a result, these radiometals often possess disparate chemical properties, thereby precluding the use of a single chemical strategy for their incorporation into radiotherapeutics. Rather, any approach to the creation of a radiometal-labeled probe must be tailored to the chemical properties of the specific metal ion. The goal of this section is to provide an overview of the coordination chemistry of the main group metals, transition metals, lanthanides, and actinides, thereby providing the reader with a foundational understanding of the radiopharmaceutical chemistry of therapeutic radiometals.

A. Hu · J. J. Wilson (✉)
Department of Chemistry and Chemical Biology, Cornell University, Ithaca, NY, USA
e-mail: jjw275@cornell.edu

6.1.1 Main Group Metals

6.1.1.1 s-Block
The s-block metals include the alkali metals (Li, Na, K, Rb, Cs, Fr) and the alkaline earth metals (Be, Mg, Ca, Sr, Ba, Ra). Among these elements, the radionuclides ^{89}Sr and ^{223}Ra are the most important candidates for RPT. Under aerobic and aqueous conditions, alkali metals attain the +1 oxidation state, and alkaline earth elements exist in the +2 oxidation state. In these oxidation states, the electron configurations of these metal ions are closed shell and match those of the nearby noble gas. These s-block metal ions are not redox-active and bind with ligands mainly via ionic rather than covalent interactions [4].

6.1.1.2 p-Block
The p-block metals include the metallic elements in Group 13 (Al, Ga, In, Tl), Group 14 (Sn, Pb), and Group 15 (Bi). Representative therapeutic radionuclides within this category are ^{67}Ga, ^{111}In, and ^{201}Tl (which are used for Auger electron therapy), as well as ^{212}Pb and ^{213}Bi (which can be used for alpha therapy). These p-block metals primarily attain two oxidation states. Their higher valent oxidation states arise from the loss of all their valence electrons, yielding a noble gas electron configuration. The lower valent oxidation state corresponds to the loss of only the valence p electrons, affording an s^2 valence electron configuration. Accordingly, these oxidation states are +3 and +1 for Group

Table 6.1 Summary of radiometals relevant to radiotherapy

	Half-life	Major decay mode	Therapeutic application
^{47}Sc	3.35 d	β^-	β therapy
^{67}Cu	61.8 h	β^-	β therapy
^{89}Sr	50.6 d	β^-	β therapy
^{67}Ga	3.26 d	electron capture	Auger electron therapy
^{90}Y	64.1 h	β^-	β therapy
^{99m}Tc	6.01 h	internal conversion	Auger electron therapy
^{105}Rh	35.4 h	β^-	β therapy
^{109}Pd	13.7 h	β^-	β and Auger electron therapy
^{111}Ag	7.45 d	β^-	β therapy
^{111}In	67.2 h	electron capture	Auger electron therapy
^{135}La	18.9 h	electron capture	Auger electron therapy
^{153}Sm	46.3 h	β^-	β therapy
^{149}Tb	4.12 h	A	α therapy
^{161}Tb	6.96 d	β^-	β and Auger electron therapy
^{166}Ho	26.8 d	β^-	β therapy
^{177}Lu	6.65 d	β^-	β therapy
^{186}Re	3.72 d	β^-	β therapy
^{188}Re	17.0 h	β^-	β therapy
^{195m}Pt	4.01 d	internal conversion	Auger electron therapy
^{198}Au	2.70 d	β^-	β therapy
^{197m}Hg	23.8 h	internal conversion	Auger electron therapy
^{201}Tl	3.04 d	electron capture	Auger electron therapy
^{212}Pb	10.6 h	β^-	α therapy[a]
^{212}Bi	60.6 min	β^-, α	α therapy[a]
^{213}Bi	45.6 min	β^-	α therapy[a]
^{225}Ac	9.92 d	α	α therapy
^{223}Ra	11.4 d	α	α therapy
^{227}Th	18.7 d	α	α therapy
^{230}U	20.8 d	α	α therapy
^{255}Fm	20.1 h	α	α therapy

[a]These radionuclides – despite their emission of β particles – are categorized as α-therapy candidates because of their α-emitting daughters

13, +2 and +4 for Group 14, +3 and +5 for Group 15. For the lighter p-block elements like Al, Ga, and In, the higher oxidation states are more stable, whereas the heavier p-block elements like Tl, Pb, and Bi tend to adopt the lower oxidation states. The larger preference of the lower oxidation states for the heavy p-block elements is a consequence of the *inert pair effect*. This concept describes enhanced stability of the s^2 electron configuration that arises from relativistic effects, which become important for the heaviest elements on the periodic table.

In many cases of p-block elements with s^2 electron configurations, the lone pair has the potential to be *stereochemically active* [5]. Complexes with a stereochemically active

lone pair—which possess what appears to be a vacant coordination site where the lone pair resides—are referred to as *hemidirected*. In some cases, however, the stereochemical activity of the lone pair is not displayed, and the coordination sphere is isotropic, resulting in a *holodirected* complex (Fig. 6.1). In any case, the possibility of lone pair stereochemical activity for the heavy p-block elements needs to be considered when exploring their radiochemistry.

6.1.2 Transition Metals

The transition metals—which belong to the d-block (Groups 3–12) of the periodic table—are

Fig. 6.1 Schematic representation of the two possible coordination modes (holodirected and hemidirected) for metal ions with an s^2 lone pair. (Reproduced from Ref. [6] with permission)
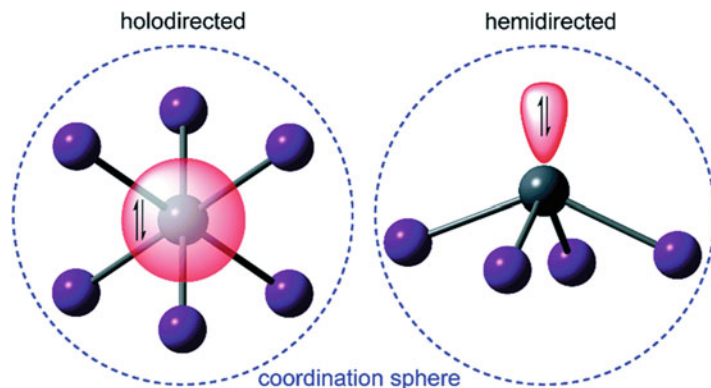
characterized by their valence *d* electrons. Representative therapeutic radiometals within this category are ^{47}Sc, ^{67}Cu, ^{90}Y, ^{99m}Tc, ^{105}Rh, ^{109}Pd, ^{111}Ag, $^{186/188}Re$, ^{195m}Pt, ^{198}Au, and ^{197m}Hg. In contrast to the main group metal ions discussed above, the *d* orbitals of transition metal ions can undergo covalent interactions with ligand donors, a property that dictates their overall geometry and stability.

Unlike the main group metal ions, the chemical behavior of the transition metal ions is highly diverse. For example, they can form cations in formal oxidation states ranging from +1 to +8 (as summarized in Fig. 6.2) and possess significantly different ligand donor atom preferences. Thus, it is challenging to summarize the chemistry of transition metal ions as a whole in a few sentences, but some underlying principles and general trends are useful for understanding how they can be employed for radiotherapeutic applications.

In general, there exist several dichotomies between the chemical properties of the transition metals. One such dichotomy is observed between the early (Groups 3–6) and late transition metals (Groups 8–12). The early transition metals are easier to oxidize, typically attaining their highest possible oxidation states by losing all their valence *s* and *d* electrons. In contrast, the late transition metals tend to form complexes with lower oxidation states. Furthermore, the cations of early transition metals are usually chemically hard and oxophilic, preferring hard ligands such as O^{2-}, F^-, and Cl^-. Their oxophilicity also

makes them susceptible to hydrolysis. The late transition metals are significantly softer and more polarizable, thus preferring soft ligands like carbonyl (CO), thiols (SR^-), and phosphines (PR_3).

Another dichotomy within the transition metals can be found by comparing those in the second and third rows to those in the first row. Most notably, complexes of the second and third row transition metal ions are significantly more inert than those of the first row metal ions. In addition, the second and third row transition metal ions tend to have more controlled redox chemistry, undergoing primarily two-electron processes with large structural reorganizations. The first row transition metal ions, in contrast, attain a wider range of oxidation states, driven by single-electron processes.

In contrast to the *s* and *p* block elements (for which electrostatic interactions predominate), there exists a high degree of covalency in the metal–ligand interactions of transition metal complexes. The bonding, electronic structure, and magnetic properties of the transition metal complexes can be rationalized in the context of *ligand field theory* [7]. Ligand field theory provides a framework for understanding how the degeneracy of the valence *d* orbitals is lifted as they interact with ligand donor orbitals to form molecular orbitals. The pattern and magnitude of the energetic splitting of the d orbitals are dependent on the geometry around the metal center, the types of ligands present, and the properties of the metal ion itself. Although multiple geometries are possible, arguably the most common one for
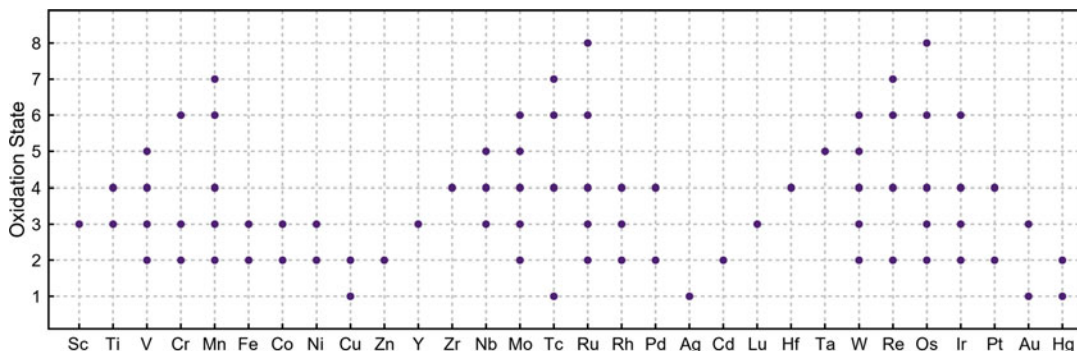
Fig. 6.2 The commonly observed oxidation states of *d*-block metal ions
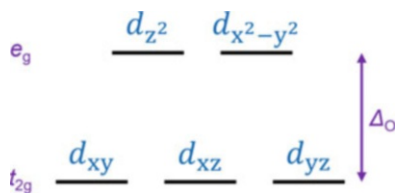
Fig. 6.3 Ligand field splitting for the valence *d* orbitals in an octahedral complex

transition metal complexes is the 6-coordinate octahedral geometry. Within this geometry, the five valence *d* orbitals are split into two energy levels, a triply degenerate t_{2g} and a doubly degenerate e_g set that are separated by an energy difference known as the *ligand-field splitting parameter* Δ_O (the subscript "O" indicates octahedral, as depicted in Fig. 6.3). The magnitude of Δ_O depends on the nature of both the metal and ligand. This quantity is important in the context of radiopharmaceutical chemistry because it reflects both the thermodynamic and kinetic stability of a transition metal complex. Generally, transition metal complexes with only the t_{2g} orbitals occupied are significantly more stable than those with electrons in the e_g orbitals, a consequence of the fact that e_g orbitals are primarily σ^* (antibonding).

6.1.3 Lanthanides

The lanthanides (Ln, the 4*f*-block) consist of the 15 elements from La to Lu in the periodic table, all of which possess stable isotopes except

Pm. Therapeutic radiometals that fall within this group include [135]La, [153]Sm, [149/161]Tb, [166]Ho, and [177]Lu. Due to similarities in their chemical properties and their cooccurrence in natural deposits, the transition metals Sc^{3+} and Y^{3+} are often categorized alongside with lanthanides, forming a larger group referred to as the "rare earth metals." In practice, chemists often use "lanthanides" and "rare earths" interchangeably. Under the aqueous and aerobic conditions required for radiopharmaceutical chemistry, the most stable oxidation state for all Ln is +3 (Ln^{3+}). This oxidation state gives rise to comparable electron configurations across the series of $[Xe]4f^n$, with $n = 0$–14. It should be noted, however, that several members of this series, particularly Ce and Eu, can be stabilized under biologically relevant conditions in +4 and +2 oxidation states, respectively, if appropriate ligands are used. The valence 4*f* orbitals of the Ln^{3+} are highly contracted and do not expand beyond the core orbitals, minimizing their spatial overlap and covalency with ligand donor orbitals. Thus, Ln^{3+}–ligand interactions are primarily ionic in nature. Ln^{3+} ions are chemically hard, preferring hard donor atoms like O and F. Although the chemical properties of Ln^{3+} ions are similar, the increasing effective nuclear charge across the series leads to a 17 pm decrease in ionic radius from La^{3+} to Lu^{3+} [8], a phenomenon described as the "lanthanide contraction" [9]. As such, the late Ln^{3+} has a larger charge-to-ionic radius ratio, which generally gives rise to more stable electrostatic interactions and stronger Lewis acidic characters.

6.1.4 Actinides

At the very bottom of the periodic table, the radioactive actinides (An, the 5f-block) comprise the 15 elements from Ac to Lr. The therapeutically relevant radioisotopes of the An series are ^{225}Ac, ^{223}Ra, ^{227}Th, ^{230}U, and ^{255}Fm. In contrast to the Ln, the valence electron configurations and preferred oxidation states of the An can vary significantly. For the early An, the 5f and 6d orbitals are of similar energy, and thus electron configurations with occupancy of both orbital types are possible. The 5f and 6d orbitals of the early An are also fairly diffuse, extending beyond the core orbital electrons. As such, the chemistry of the early An (Ac–Pu) somewhat resembles that of transition metals in that the 5f and 6d orbitals can participate in covalent bonding with ligand atoms, and these ions can attain multiple oxidation states. The major oxidation states for these elements are Ac(III), Th(IV), Pa(V), U(VI, IV), Np(V), and Pu(IV). Within these early An, metal–ligand multiple bonding is possible and has particularly important implications for the coordination chemistry of Pa^{5+} and U^{6+}. Indeed, the major forms of these metals under aerobic aqueous conditions are the $[Pa^V{\equiv}O]^{3+}$ and $[O{\equiv}U^{VI}{\equiv}O]^{2+}$ (uranyl) cations. Similarly, Np and Pu can exist in $[O{\equiv}Np^V{\equiv}O]^+$ (neptunyl) and $[O{\equiv}Pu^{VI}{\equiv}O]^{2+}$ (plutonyl) forms. The unique linear geometry of these species needs to be considered when harnessing them in RPT.

As the effective nuclear charge and relativistic effects increase across the series, the 5f orbitals become significantly stabilized and contracted relative to the 6d orbitals such that all valence electrons occupy the former. In the late An, this 5f orbital contraction precludes significant covalent interactions with ligand donor atoms. As such, the late An ions have similar chemical properties to the Ln, forming ionic complexes and existing primarily in +3 oxidation states. However, due to their extremely limited availability and poorly understood chemistry, these metals currently have limited relevance to RPT; only ^{255}Fm has been proposed as a potential candidate. Further efforts to increase their availability and characterize their chemical properties are needed before they can be strongly considered for applications in nuclear medicine.

6.2 The Details: Converting Metallic Radionuclides into Radiopharmaceutical Agents

Both the chemical properties of the radiometal and the desired targeting strategy must be considered prior to the implementation of radiometals into radiopharmaceuticals. In the ensuing section, several different approaches for incorporating radiometals into radiopharmaceuticals are described. Although this book and this chapter are focused on agents for RPT, the principles described also apply to the construction of radiometallated imaging agents.

6.2.1 Standalone Inorganic Salts

Occasionally, free, uncomplexed radiometal ions have properties that are suitable for their standalone use in medicine. This type of application is possible when the radiometal ion has a natural affinity for a specific tissue or organ. In the context of RPT, this phenomenon most frequently manifests in the form of metal ions with bone-seeking properties that facilitate their localization in regions of high bone turnover like bone metastases [10]. Key examples are the alkaline earth radiometals $^{89}Sr^{2+}$ and $^{223}Ra^{2+}$, both heavier analogues of Ca^{2+} (a major constituent of bone matrix). $[^{89}Sr]SrCl_2$ (Metastron™) has been prescribed for the palliative treatment of skeletal metastases [11], and $[^{223}Ra]RaCl_2$ (Xofigo®) is currently used for the management of bone metastases in castration-resistant prostate cancer patients [12] (see Chap. 19 for more details).

6.2.2 Metal–Ligand Complexes

Despite the clinical success of the examples described above, the use of free radiometal ions

for therapeutic applications is very limited because most radiometals do not display inherently useful biodistribution patterns. Indeed, most free radiometal ions accumulate in undesired tissues or organs, giving rise to toxic side effects. Thus, the majority of therapeutic radiometals require the use of ligands to control their chemical and biological properties. Carefully chosen ligands can produce complexes with a number of valuable properties and circumvent the toxic side effects associated with free radiometal ions. In addition to preventing toxicity, the ligands can also be leveraged to enhance tumor-targeting properties. The rational design of ligands with vectors for targeting receptors that are overexpressed on cancer cells is a hallmark of RPT. Finally, before moving on it is important to note that metal ions are almost always bound by ligands in solution. For example, "free" metal ions in an aqueous solution actually form coordination complexes with H_2O molecules. However, in this discussion, we only consider exogenously added ligands.

6.2.2.1 Metal Complexes with a Chelator

Different types of ligands can be used to bind medicinally relevant radiometal ions. Chelating agents—or chelators—are a particularly relevant subset. This class of ligands is generally defined by the presence of multiple donor atoms within a single compound. Although simple bidentate ligands (e.g., ethylenediamine) are chelators in the strictest sense, radiopharmaceuticals typically require chelators with significantly more donor atoms to maximize the thermodynamic and kinetic stability of the resulting complexes. Thus, radiopharmaceutical researchers usually use the word "chelator" to refer to a ligand that provides sufficient donor atoms to enable the formation of a 1:1 complex with the metal ion.

Chelators are effective in radiopharmaceuticals because their multidentate nature leads to the formation of complexes with high thermodynamic and kinetic stability. To elaborate, the ability of a single chelator molecule to bind ions with several donors gives rise to the *chelate effect*, a phenomenon that results in

chelators yielding more stable complexes than those formed by an identical number of analogous monodentate donors [13]. The chelate effect is primarily driven by entropy; the displacement of several monodentate exogenous ligands by a single multidentate chelator is entropically favorable. Moreover, there is a kinetic element in play as well; because the donor atoms of a chelator are confined to the same molecule, the coordination of one donor atom within a chelator makes the coordination of others more kinetically facile.

The suitability of different chelators for therapeutic radiometals can be assessed quantitatively via several experiments. A number of these experiments can be carried out using nonradioactive or longer-lived isotopes of the radiometal of interest, which reduces both their cost and attendant safety considerations. However, differences between the concentrations needed to work at the macroscopic scale with these stable or longer-lived surrogates and the radioisotopic scale with the actual therapeutic radionuclides can, in some cases, give rise to disparities in the efficacy of chelators.

(a) *Facile complex preparation*

Operations involving radionuclides are inherently time sensitive due to their continuous decay. Ideally, the formation of a desired radio metal–ligand complex—*a.k.a.* "*radiolabeling*"— needs to be accomplished in a facile and rapid manner. Although harsh conditions such as higher temperatures can be used to accelerate radiolabeling reactions, the sensitivity of some radiopharmaceutical targeting vectors (like immunoglobulins) precludes heating.

In a typical chelator radiolabeling reaction, the radiometal and chelator are incubated at a well-defined temperature and pH for a pre-set reaction time. The efficiency of this radiolabeling reaction is often described by the *radiochemical conversion* (RCC), which is the percentage of the initial total radioactivity incorporated into the chelator (after correcting for the physical decay of the radionuclide over the course of the experiment). The *radiochemical yield* (RCY), the overall percent of incorporated radioactivity after additional

reaction workup procedures like purification, is another important parameter that can also depend on the chelator. Generally, an excess of the chelator is used to maximize both parameters. The success of a radiolabeling reaction is also often assessed in terms of the amount of radioactivity incorporated per mol or per gram of the chelator, values referred to as the *apparent molar activity* (AMA) or *apparent specific activity* (ASA), respectively. The production source and batch of the radionuclide can also affect the RCC, RCY, and AMA/ASA, as the presence of even small amounts of metal ion impurities can dramatically affect the radiolabeling reaction (see Chap. 8).

(b) *Sufficient complex stability*

Beyond allowing for efficient radiolabeling, a chelator must also form a sufficiently stable complex with the radiometal to prevent its release from the radiopharmaceutical vector in vivo. In principle, both the thermodynamic and kinetic stability of a radiometal–chelator complex should be measured and considered.

(i) Thermodynamic stability

The *thermodynamic stability* of a metal–ligand complex describes the spontaneity of the binding process between the two components. Thermodynamic stability is quantified by the standard free energy change of complexation ($\Delta G°$) and the stability constant (K_{ML}), which are explicitly related to each other. K_{ML} values are used more often due to their more easily interpreted definition. K_{ML} is defined in Eq. 6.1, in which [M], [L], and [ML] are the concentrations of the free metal ion, free ligand in its fully deprotonated state, and metal−ligand complex, respectively, at chemical equilibrium. From this expression, it is clear that a larger K_{ML} indicates stronger binding, which leads to smaller concentrations of the free metal ion at equilibrium. Thus, this quantity is highly useful for assessing ligands in a wide array of research areas [14].

$$K_{ML} = [ML]/[M][L] \qquad (6.1)$$

K_{ML} is a pH-independent quantity, as [L] represents the concentration of the fully deprotonated form of the chelator. Under the aqueous and aerobic conditions relevant to radiopharmaceutical chemistry, H^+ competes with the metal ion to bind to the ligand donor atoms, and OH^- competes with the ligand to hydrolyze the metal center. Thus, the pH of the solution plays an important role in the thermodynamic stability of the complex. As such, *conditional stability constants*—defined at specific pH values—are useful as well. An extension of this concept is the pM value. The pM of a metal–chelator combination is defined as $-\log [M]_{free}$, where the total metal concentration c_M is 10^{-6} M, and the total ligand concentration c_L is 10^{-5} M, at pH 7.4 [15]. Using this scale, large pM values signify smaller quantities of free metal ion present under these conditions and thus reflect more thermodynamically stable chelators at physiological pH.

(ii) Kinetic stability

Although thermodynamic stability quantities K_{ML} and pM are useful for comparing and understanding the metal ion affinity and selectivity of chelators at equilibrium, these values do not contain any information regarding the *rate* of the formation or dissociation of the metal–chelator complex. These parameters fall into the domain of *chemical kinetics*: the study of the rate of chemical reactions. In the context of the stability of a radiometal–chelator complex, the rate of dissociation is an important parameter. The *kinetic stability* (or *inertness*) of a metal–ligand complex describes the dissociation rate of the complex under a thermodynamically unfavored condition. It should be noted that the thermodynamic and kinetic stabilities of metal complexes do not necessarily correlate. In the context of RPT, the kinetic stability of a complex is critical because the conditions encountered in vivo—dilute concentrations of the metal–ligand complex in the presence of much higher concentrations of endogenous competing metal ions and ligands—often lead to unfavorable

thermodynamics. However, the kinetic stability of a radiometal complex is difficult to directly and absolutely quantify. Researchers often employ challenge experiments to assess this property, and three of the most frequently used methods are described below. These methods can be adapted for use with cold or radioactive metal ion complexes by altering the techniques used to determine the dissociation rates of the complexes.

Under low pH conditions, the high H^+ concentrations generally favor the protonation of the chelator and the displacement of the metal ion from a thermodynamic perspective. In such an *acid challenge* experiment, the complex is placed in a strongly acidic condition, and the dissociation kinetics are monitored for the evaluation of complex kinetic stability. Similarly, an excess of competing chelators can be used to create thermodynamically unfavored conditions for the original metal–chelator complex. The pseudo-first-order rate constant for this *transchelation challenge* process can afford a measure for the inertness of the initial complex. Following the same principle, a competing metal ion can also be used for a *transmetallation challenge*, in which an excess of a competing metal is added to displace the original metal, enabling the determination of a pseudo-first-order rate constant for the dissociation of the original complex.

A key similarity of the kinetic studies described above is that none provides an absolute value for this property. In each case, the rate constants obtained are dependent on the experimental conditions, including the concentrations of reagents, pH, and temperature. Thus, these values can only be used in a comparative manner when different complexes are subjected to identical conditions. Hence, it is prudent to benchmark these experiments using a well-known system when probing the inertness of novel metal–chelator complexes.

(c) *Conjugation with targeting vector*

Once the radiolabeling efficiency and complex stability have been verified for a radiometal–chelator complex, the next step is the development of approaches for attaching the chelator to the targeting vector. There are a few examples of nontargeted radiometal complexes that are used as radiopharmaceuticals, like [^{153}Sm]Sm–EDTMP (Quadramet®, Fig. 6.5) that is used for the treatment of bone metastases [16]. However, most chelator-based radiopharmaceuticals include a targeting vector that is relied upon to deliver the radiometal to tissues in vivo.

Figure 6.4 reflects a general workflow for constructing a chelator-based radiopharmaceutical. After a chelator is revealed to be chemically promising, a derivative of the chelator containing a reactive functional group—a *bifunctional chelator*—is designed and synthesized. This bifunctional chelator is then allowed to react with a targeting vector containing a reactive group, which can be either natural (such as a thiol of cysteine or a primary amine of lysine) or synthetic (such as an azide or an alkyne), a step called *conjugation*. This chelator-modified conjugate is then radiolabeled to yield the completed radiopharmaceutical. Typically, the conjugation of the bifunctional chelator precedes the radiolabeling step because it minimizes the time of handling radioactive materials. Under some circumstances, however, radiolabeling is required *before* the chelator conjugation step. For
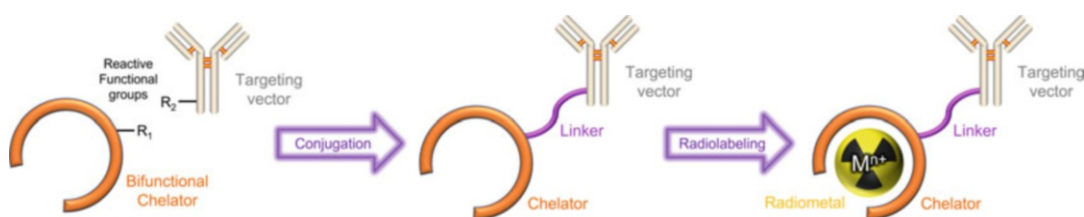
Fig. 6.4 General strategy for the construction of a metal-chelate-based radiopharmaceutical agent
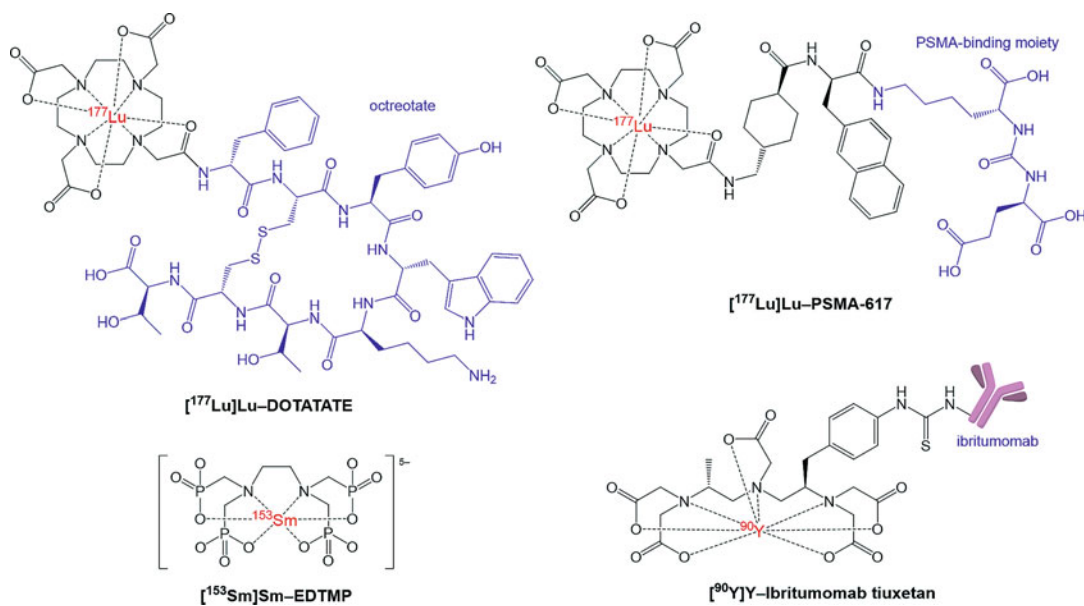
Fig. 6.5 Approved radiometal-based therapeutic agents that use chelators

example, if a high temperature is required for the radiolabeling but the vector is heat-sensitive, the bifunctional chelator needs to be radiolabeled before its attachment to the vector.

The suitability of a chelator in RPT should take into account the synthetic ease with which its bifunctional analogue can be prepared. Moreover, the installation of a reactive functional group to make the bifunctional chelator can potentially alter its metal-binding properties. In some cases, the parent chelator efficiently forms stable radiometal complexes, but its bifunctional analogue or corresponding conjugate does not. Thus, the chelating efficacy should be assessed again after the targeting vector is introduced. These challenges highlight the many different factors that need to be considered during the development of a chelator- and radiometal-bearing radiopharmaceutical.

A variety of molecules can act as targeting vectors. These compounds can be small molecules, short peptides, and macromolecular antibodies or antibody fragments. For instance, the small-molecule moiety Glu–urea–Lys binds to the prostate-specific membrane antigen (PSMA), a zinc glycoprotein that is overexpressed by prostate cancer cells [17]. This

targeting vector has been employed in [^{177}Lu]Lu–PSMA-617 (Pluvitco®, Fig. 6.5), a newly approved drug for the treatment of metastatic castration-resistant prostate cancer [18] that is described in more detail in Chap. 18. Another ^{177}Lu-based RPT agent, [^{177}Lu]Lu-DOTATATE (Lutathera®, Fig. 6.5) [19], is based on a peptide that targets the somatostatin receptor that is frequently overexpressed by gastroenteropancreatic neuroendocrine tumors [20]. A final example of an RPT agent, the non-Hodgkin lymphoma drug [^{90}Y]Y-ibritumomab tiuxetan (Zevalin®, Fig. 6.5) [21], employs the macromolecular monoclonal antibody ibritumomab to target the CD20 antigen expressed on B lymphocytes [22]. These three examples highlight how different types of targeting vectors can be successfully applied in radiotherapeutics, topics that are discussed in a great detail in Chaps. 9, 10, 11, 12, 13, 14, 15, 16, 17, 18, and 19.

(d) *Well-known chelators*

Generally speaking, chelators are classified as either macrocyclic or acyclic. Acyclic chelators have an open-chain or linear structure, whereas macrocyclic chelators have (as their name suggests) a cyclic structure, typically with at

least nine atoms and three donor atoms in their backbones [23]. Several generalizations can be used to compare these two classes of chelators, though they do not necessarily hold true for all systems.

Macrocyclic chelators, unlike acyclic systems, benefit from the *macrocyclic effect*. This effect stems from the restricted conformational freedom of the chelator's cyclic backbone, which gives the chelator a preorganized cavity for the metal. This preorganization diminishes the entropic penalty for complex formation, thus enhancing the thermodynamic stability of complexes formed with macrocyclic chelators when compared to their acyclic analogues [24]. The macrocycle 18-crown-6 provides a key example of this phenomenon. It binds K^+ with high affinity and selectivity compared to linear polyethers. In addition to this thermodynamic advantage, macrocycles also tend to confer complexes with enhanced kinetic inertness due to their conformational inflexibility. A potential limitation of macrocyclic chelators, however, lies in their relatively slow complex formation kinetics, which sometimes necessitates harsh radiolabeling conditions like elevated temperatures.

Acyclic chelators, in contrast, typically form metal complexes rapidly and therefore require milder radiolabeling conditions. From a synthetic chemistry standpoint, the formation of macrocycles is often challenging and low-yielding, whereas acyclic chelators are often easier to synthesize. In many cases, the benefits conferred by the macrocyclic effect cannot be justified in the context of the effort required to prepare macrocycles, especially when an acyclic analogue performs well enough.

Several chelators that have been used extensively in radiopharmaceutical applications are shown in Figs. 6.6 and 6.7. Among them, the macrocyclic 1,4,7,10-tetraazacyclododecane-1,4,7,10-tetraacetic acid (DOTA) [25] and the acyclic diethylenetriaminepentaacetic acid (DTPA) have arguably been used most. Indeed, nearly all approved metal-chelate-based therapeutic and diagnostic agents are derivatives of these two structures.

DOTA (Fig. 6.6) contains a 12-membered macrocyclic cyclen ring with four pendant acetate donor arms. The rigid macrocycle and eight donor atoms of DOTA allow it to form highly inert complexes. The efficacy of DOTA has been demonstrated with a wide range of radionuclides, including the therapeutic $^{47}Sc^{3+}$, $^{90}Y^{3+}$, $^{177}Lu^{3+}$, and $^{225}Ac^{3+}$. Building upon the success of DOTA, a number of derivatives of this chelator—including DO3A, TCMC, DOTMP, and PCTA (Fig. 6.6)—have been synthesized. Close analogs of DOTA are currently used in several clinically approved radiopharmaceuticals, including [^{177}Lu]Lu–DOTATATE and [^{177}Lu]Lu–PSMA-617 (Fig. 6.5). Yet despite its clinical success, DOTA's poor metal-binding kinetics represent a notable limitation. To wit, high temperatures are typically required for efficient radiolabeling. Thus, care must be taken when this chelator is used in conjunction with temperature-sensitive biomolecules.

The solution conformational equilibrium of DOTA complexes has been heavily investigated and discussed over the last few decades. DOTA complexes can adopt two conformations: square antiprismatic (SAP) and twisted square antiprismatic (TSAP), both of which possess a C_4 rotation axis. These two isomers are a consequence of the different conformational chiralities that arise upon metal binding. As illustrated in Fig. 6.8a, the five-membered chelate rings can adopt either δ or λ conformations, depending on their tilt directions. In the most energetically favorable forms, the four chelate rings assume the same conformations, yielding a $\delta\delta\delta\delta$ or a $\lambda\lambda\lambda\lambda$ arrangement in the resulting complex. In addition, the four pendant acetate donors of DOTA assume a chiral helical twist about the metal center, which is denoted as being in either a right-handed (Δ) or left-handed (Λ) conformation. Considering these conformational chiralities, four stereoisomers are possible for DOTA complexes: $\Delta(\delta\delta\delta\delta)$, $\Delta(\lambda\lambda\lambda\lambda)$, $\Lambda(\delta\delta\delta\delta)$, and $\Lambda(\lambda\lambda\lambda\lambda)$. The enantiomeric pair $\Delta(\lambda\lambda\lambda\lambda)$ and $\Lambda(\delta\delta\delta\delta)$ result in the SAP conformer, whereas the enantiomeric pair $\Delta(\delta\delta\delta\delta)$ and $\Lambda(\lambda\lambda\lambda\lambda)$ give rise to the TSAP conformer (Fig. 6.8b). These two
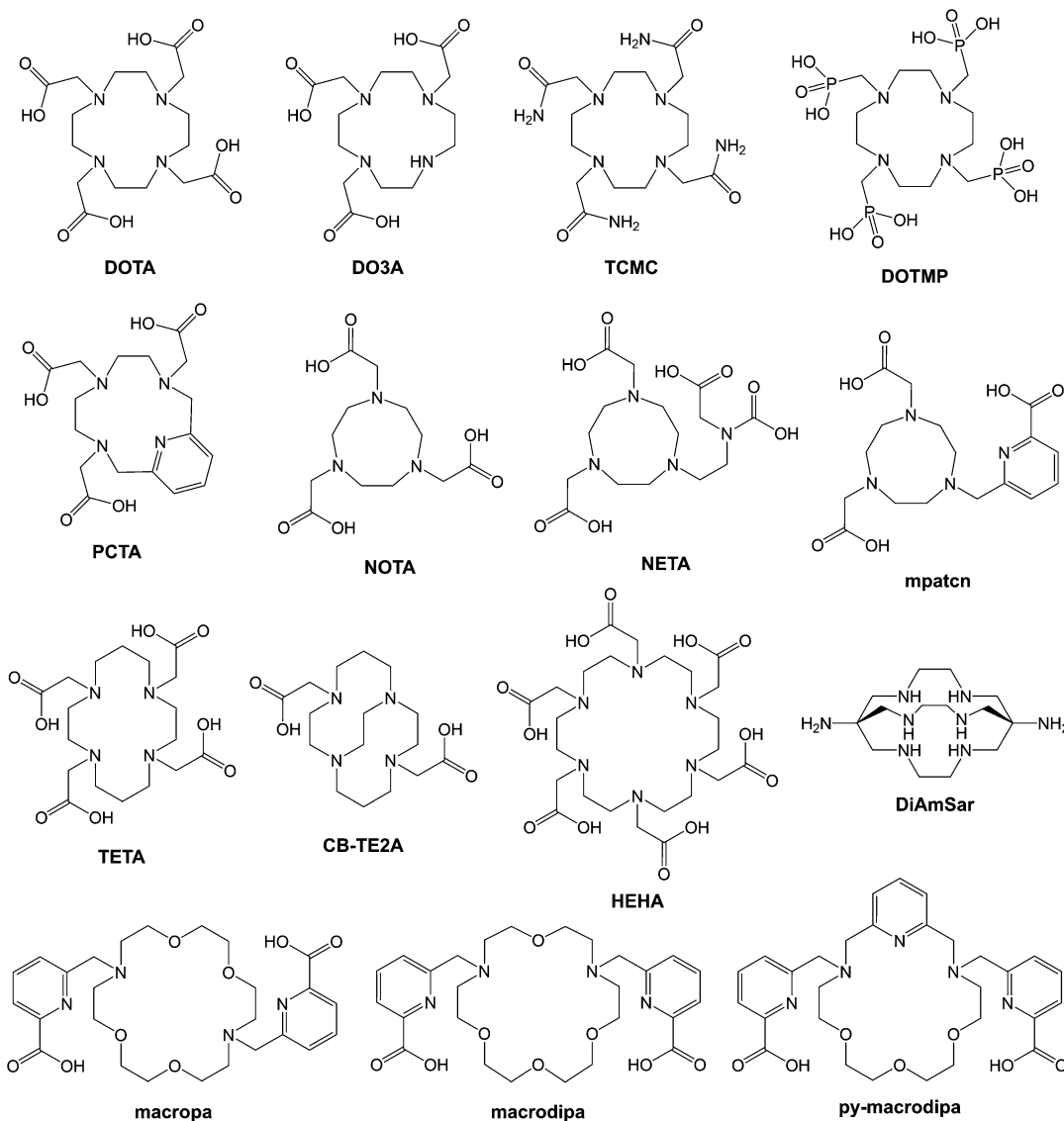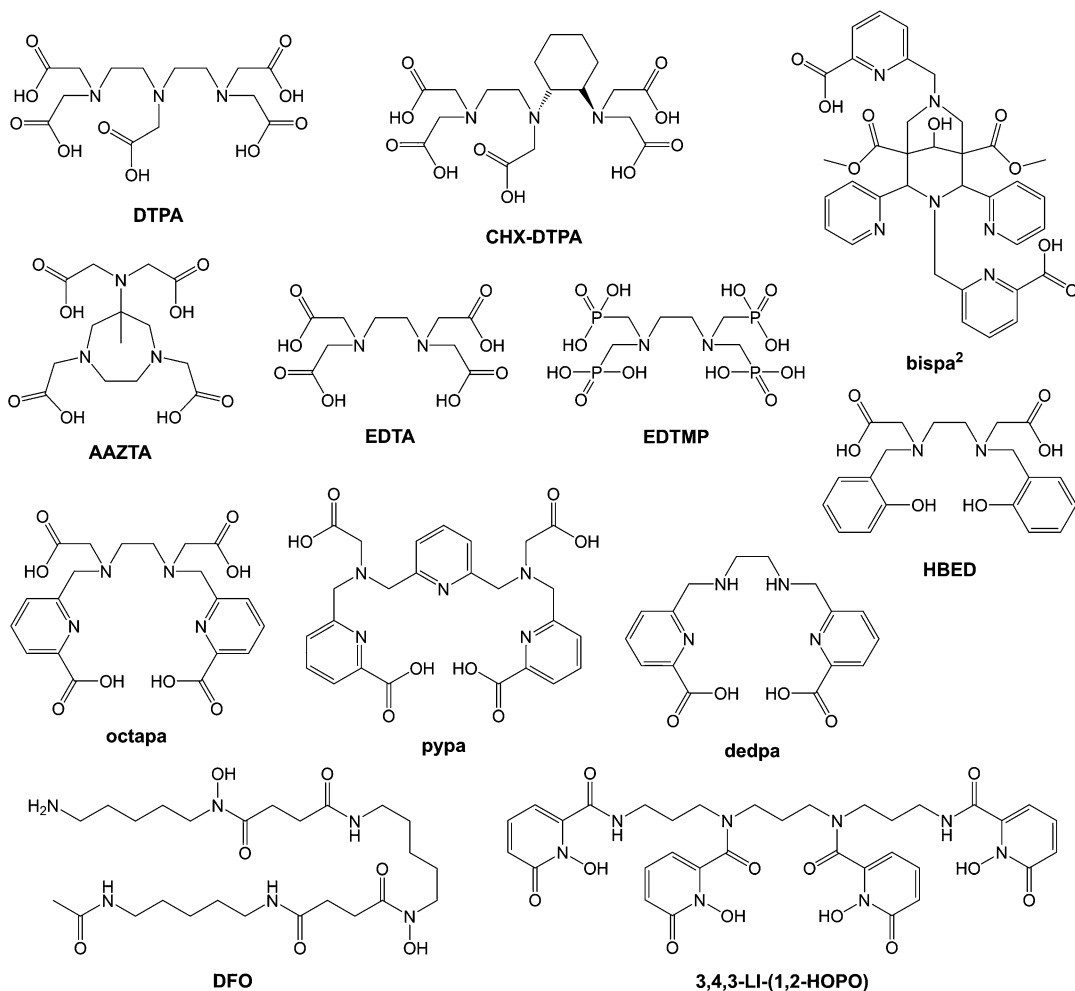
Fig. 6.6 Selected macrocyclic chelators used in the development of radiopharmaceuticals

conformers can interconvert by either an arm rotation or a ring inversion. Generally, the TSAP conformer is usually adopted in thermodynamically less stable complexes of larger ions like La^{3+}, whereas the SAP conformer is preferred for highly stable complexes of smaller ones like Lu^{3+}.

DTPA (Fig. 6.7) is an acyclic chelator with five acetate arms attached to a diethylenetriamine backbone, affording three N donors and five O donors. DTPA is one of the earliest chelators to be applied in radiopharmaceutical chemistry.

Extensive research on the coordination chemistry of DTPA has been undertaken, and this chelator has been revealed to rapidly radiolabel several therapeutic radionuclides under mild conditions, including $^{47}Sc^{3+}$, $^{90}Y^{3+}$, and $^{177}Lu^{3+}$ [26]. A clinical RPT agent that employs an analogue of DTPA is [^{90}Y]Y–ibritumomab tiuxetan (Zevalin®, Fig. 6.5), which is approved for the treatment of non-Hodgkin's lymphoma [21].

Despite their favorable radiolabeling chemistry, DTPA complexes often experience in vivo stability issues due to their structural flexibility.

Fig. 6.7 Selected acyclic chelators used in the development of radiopharmaceuticals

Thus, recent efforts have focused on the development of analogues of DTPA that form more inert complexes. One such derivative is CHX-DTPA (Fig. 6.7), which contains a *trans*-diaminocyclohexyl group fused into the backbone. With this rigid group in place, the conformational flexibility of this linear chelator is significantly diminished compared to DTPA, thereby conferring it with a much higher degree of preorganization and giving rise to complexes with greater kinetic stability than those of DTPA. This example highlights a strategy that is commonly applied to improve the kinetic stability of a chelator: the incorporation of rigid moieties into the ligand backbone.

A benzyl isothiocyanate was attached to the backbone of CHX-DTPA, to convert it into a bifunctional chelator. By introducing this group, however, a new chiral center is generated that adds to the existing two chiral centers of the *trans*-diaminocyclohexyl group. Consequently, four possible stereoisomers—the enantiomeric pair CHX-A′-DTPA and CHX-A″-DTPA, as well as the enantiomeric pair CHX-B′-DTPA and CHX-B″-DTPA—are created (Fig. 6.9). These enantiomeric pairs are further distinguished upon their conjugation to chiral targeting vectors, thereby affording four diastereomers with different chemical properties and metal complex stabilities. The Y^{3+} complex of CHX-A-
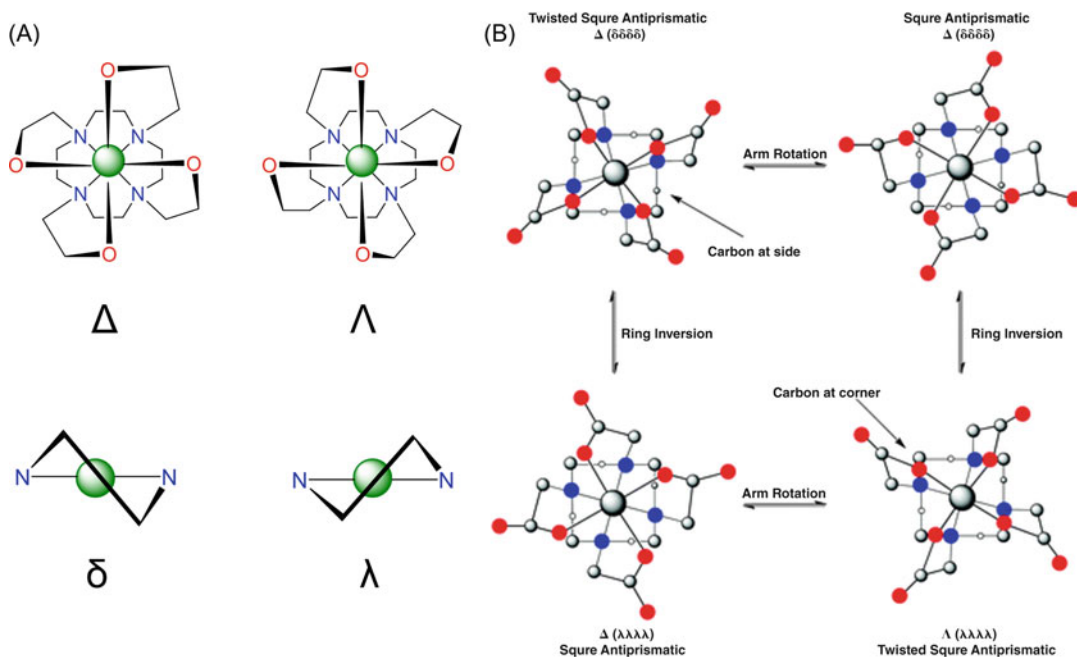
Fig. 6.8 (**a**) Depiction of the sources of chirality in DOTA complexes. (**b**) The stereoisomeric equilibrium for DOTA complexes in solution. (Reproduced from Ref. [25] with permission)

DTPA was found to be significantly more stable than that of CHX-B-DTPA. In an in vivo study in which the four stereoisomers were conjugated to a monoclonal antibody and then radiolabeled with $^{88}Y^{3+}$, the four radioimmunoconjugates exhibited different stability and biodistribution profiles, resulting in different degrees of $^{88}Y^{3+}$ accumulation in the bone with the CHX-B-DTPA analogues displaying more bone uptake than the CHX-A-DTPA complexes [27]. The development of the bifunctional variants of CHX-DTPA demonstrates that subtle structural changes can exert a significant influence on the stability of metal complexes.

(e) *Chelators for large radiometals*

The majority of chelators—such as those shown in Figs. 6.7 and 6.8—preferentially bind and stabilize smaller metal ions. The poor efficacy of these chelators for large radiometals is most likely a consequence of their small cavity sizes and the more charge-diffuse nature of large

metal ions that weakens the electrostatic interactions with the ligand donor atoms [28]. Although these types of chelators have been useful for many radiometal ions, large radiometals with promising therapeutic applications have been identified in recent years. For these reasons, there have been substantial efforts to design chelators with a preference for large over small metal ions.

The use of chelators with large macrocycles was found to be an effective strategy for coordinating large radiometal ions. Specifically, macrocyclic chelators containing 1,7-diaza-18-crown-6 were discovered to possess *reverse size selectivity*, a property that describes their greater affinity for large over small metal ions. Among this class of chelators, macropa (Fig. 6.6) has arisen as a promising candidate for RPT. The reverse size selectivity of macropa is demonstrated by its K_{ML} values (Fig. 6.10) with the lanthanides (Ln^{3+}) [29] and alkaline earth metals [30], two classes of metal ions with similar chemical properties but different ionic radii.
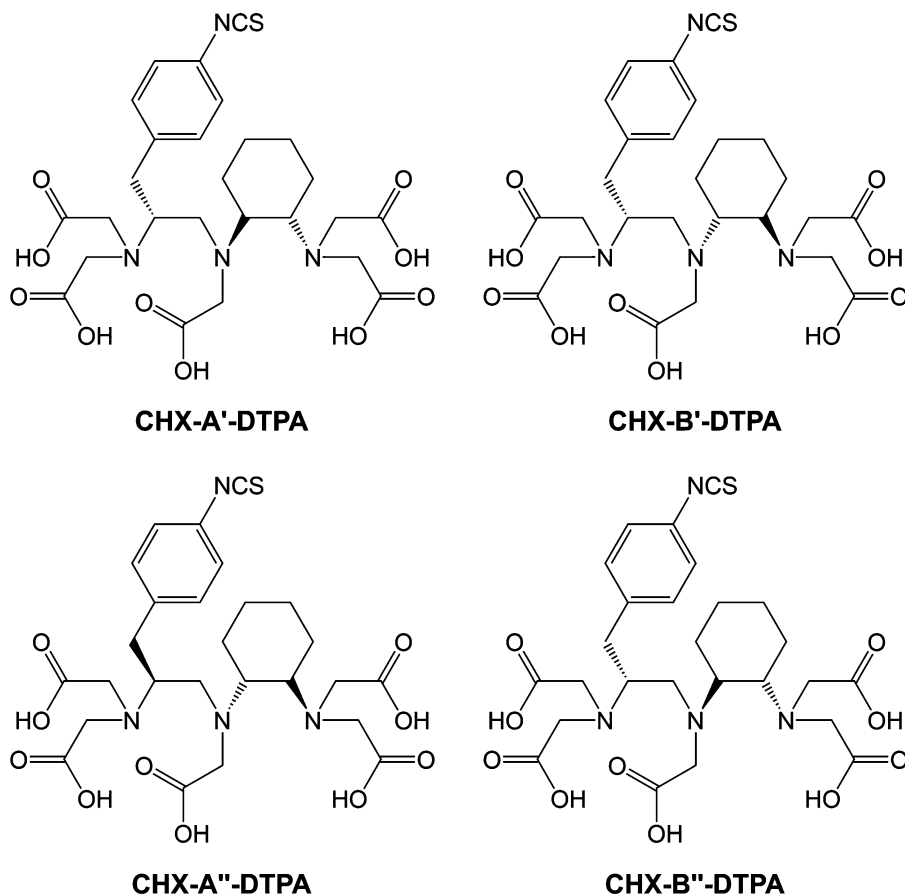
Fig. 6.9 Structures of CHX-A′-DTPA, CHX-A″-DTPA, CHX-B′-DTPA, and CHX-B″-DTPA

Given its high affinity for large metal ions, macropa has been established as an effective chelator for several large radiometals, including $^{135}La^{3+}$, $^{213}Bi^{3+}$, $^{223}Ra^{2+}$, and $^{225}Ac^{3+}$ [28].

(f) *Chelators for both large and small radiometals*

Despite the efficacy of reverse-size-selective chelators with large radiometals, their poor affinity for small radiometals limits their versatility. Recently, a new class of chelators with *dual size selectivity*—a property that reflects a high affinity for both large and small radiometals—was developed. The macrocyclic chelators macrodipa and py-macrodipa (Fig. 6.6) are members of this class, as reflected by the trends in their log K_{ML} values across the Ln^{3+} series (Fig. 6.11a)

[31, 32]. This unique property is a consequence of their ability to toggle between two distinct conformations and thus accommodate both large and small metal ions. Large Ln^{3+} form complexes in the distorted C_2-symmetric, 10-coordinate conformation A, whereas small Ln^{3+} sit in the asymmetric, 8-coordinate Conformation B, as depicted in Fig. 6.11b. In particular, py-macrodipa has been revealed to efficiently form inert complexes with the large therapeutic radionuclides $^{135}La^{3+}$ and $^{213}Bi^{3+}$ as well as the small diagnostic radiometal $^{44}Sc^{3+}$.

6.2.2.2 Metal Complexes with Multiple Low-Denticity Ligands

An alternative approach to chelators is the use of an array of simpler ligands of lower denticity to form coordination complexes. Because lower-

Fig. 6.10 Stability constants of complexes formed by macropa with lanthanide and alkaline earth metal ions plotted versus ionic radii. These plots show the reverse size selectivity of macropa. (Metal ionic radii are taken from Ref. [8])
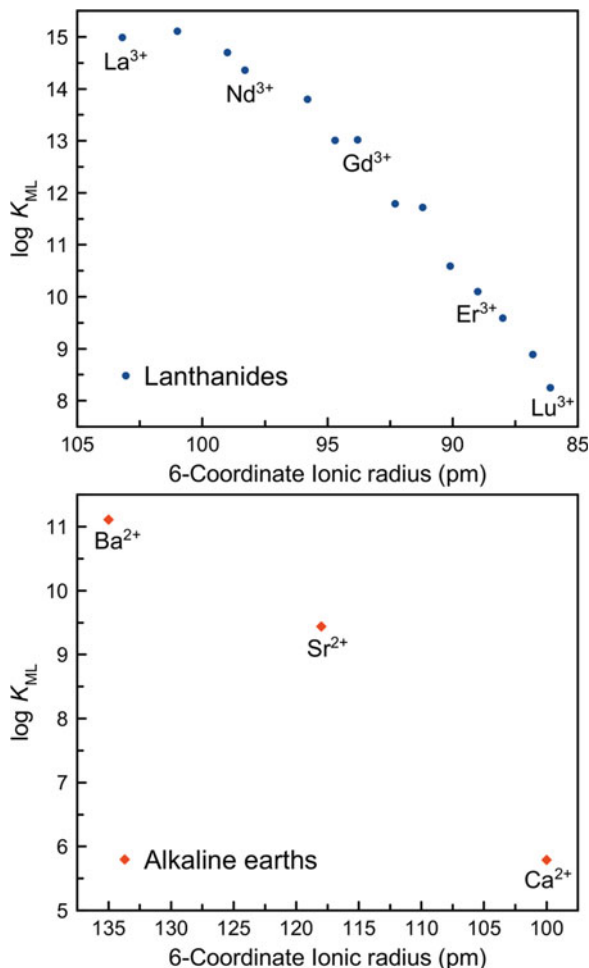

denticity ligands are more dynamic and labile, this strategy can only be applied to radiometal ions that are intrinsically capable of forming inert covalent metal–ligand interactions. These radiometal ions predominately fall within the transition metal series for which ligand field stabilization effects produce inert complexes. Like the chelator strategy described above, this approach requires that the desired radiometal complex be stable in vivo and can be formed with a high specific activity.

The best example of this approach employs ^{99m}Tc. Although this radionuclide has been recently investigated for its potential in Auger electron therapy, it is conventionally used as a diagnostic γ-ray emitter for single-photon emission computed tomography (SPECT). Relatively simple coordination and organometallic complexes of this radiometal are sufficiently stable for in vivo applications, and many ^{99m}Tc-containing complexes have been approved for clinical use. For example, the homoleptic octahedral complex [^{99m}Tc]Tc(I)–sestamibi (Cardiolite®, Fig. 6.12) contains six monodentate methoxyisobutylisonitrile ligands and is sufficiently stable for use as an SPECT imaging agent in cardiology [33]. Furthermore, tricarbonyl complexes of ^{99m}Tc that contain three monodentate carbonyl (CO) ligands are also highly robust in vivo. Like ^{99m}Tc, ^{195m}Pt has also primarily been investigated for SPECT applications but has recently been recognized as a potential radionuclide for Auger-electron-mediated therapy. The intrinsic inertness of Pt^{2+}

Fig. 6.11 (**a**) Stability
constants versus ionic radii
plotted for rare-earth
complexes formed by
macrodipa and
py-macrodipa. These plots
show their dual size
selectivity. (Metal ionic
radii are taken from Ref.
[8]). (**b**) A graphical
representation of the
conformational toggle of
this ligand class upon
binding large
(Conformation A) and
small (Conformation
B) ions
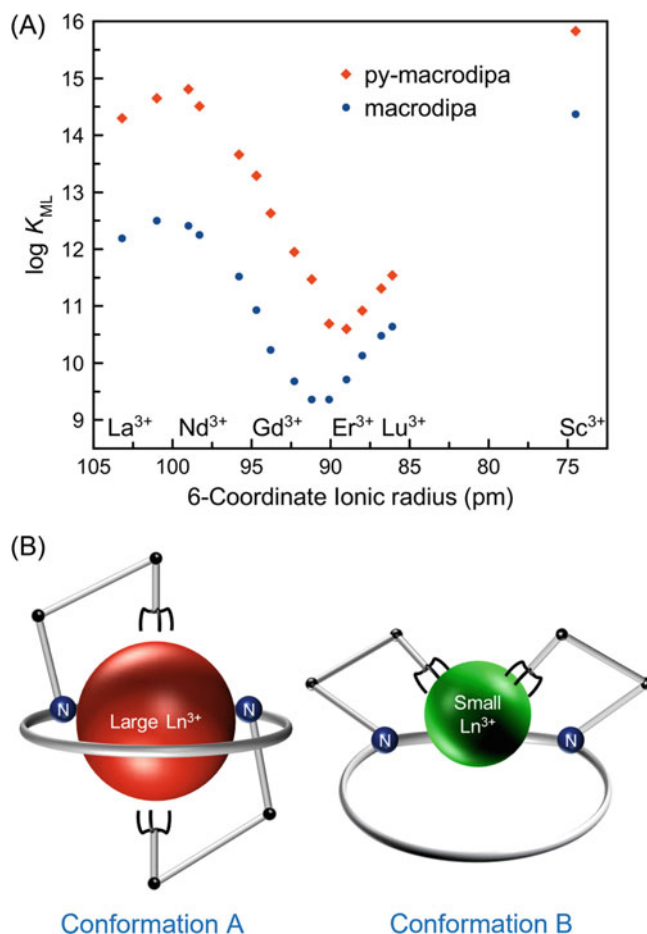
Fig. 6.12 The transition-
metal-based
radiopharmaceuticals
discussed in this chapter
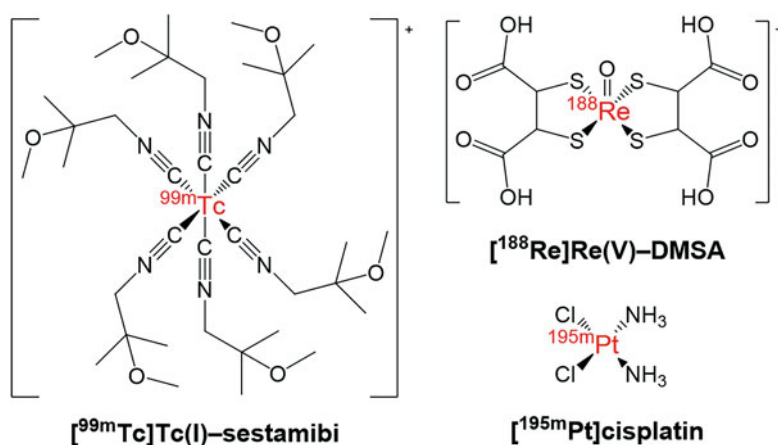
has enabled the assembly of [195m]Pt-based
radiopharmaceuticals with simple monodentate
ligands. A key example is the preparation of
[195m]Pt-labeled cisplatin (Fig. 6.12), which

contains monodentate ammine and chloride
ligands. This labeled compound was ~85% more
effective at inhibiting tumor growth compared to
nonradioactive cisplatin, demonstrating the

therapeutic potential of the Auger electron emissions of ^{195m}Pt [34].

In principle, this coordination strategy could be employed with other therapeutic radioisotopes of transition metals that preferentially form covalent bonds with ligands, such as the β-emitters $^{186/188}$Re, ^{109}Pd, and ^{105}Rh. Because Re is the heavier Group 7 congener of Tc, the chemistry of these two elements is similar, allowing for radiolabeling strategies employed with ^{99m}Tc to be used for therapeutic $^{186/188}$Re-labeled analogues [35]. For example, [^{99m}Tc]Tc(V)–DMSA (NephroScan™)—in which DMSA is the bidentate ligand *meso*-2,3-dimercaptosuccinic acid—is used for the scintigraphic evaluation of renal parenchymal disorder, whereas its analogue, [^{188}Re]Re(V)–DMSA (Fig. 6.12), has been investigated for RPT. This ^{188}Re complex was tested in prostate cancer patients with disseminated bone metastases and produced high uptake in these malignant lesions but also undesired high renal accumulation [36]. Another low-denticity ligand, the bisphosphonate etidronic acid (1-hydroxyethylidene-1,1-diphosphonic acid, HEDP), has been used in the radiopharmaceutical agent [^{186}Re]Re–HEDP (Etidronate®) for the palliative treatment for bone metastases. Although this drug was approved in Europe, it has since been withdrawn from the market in this region and is currently only found in developing countries.

The major advantage of using these simple low-denticity ligands is that they do not require the lengthy multistep organic syntheses that are often necessary to obtain multidentate chelators. In general, however, it can be argued that chelators are still preferable to lower-denticity ligands for RPT for several reasons. First, the chelate and (in some cases) macrocyclic effects enable chelators to form more stable complexes than lower-denticity ligands. Furthermore, the use of chelators for radiopharmaceutical applications is more widespread across the entire periodic table. Simpler ligands can only be used with transition metal ions that have *d* electron configurations that permit the formation of highly inert complexes. In addition, radiolabeling processes involving chelators are typically more straightforward than those involving multiple simple ligands. Whereas the formation of a radiometal–chelator complex only requires mixing the two components, the formation of coordination complexes with lower-denticity ligands often necessitates other components to modulate the redox state of the metal. Finally, lower-denticity ligands potentially give rise to complexes with constitutional isomers that can have different biological properties.

6.2.3 Nanoparticles

The use of nanoparticles in medicine has expanded significantly over the past several decades. Nanoparticles are generally defined by their size: at least one dimension to be between 1 and 100 nm. A number of properties of nanoparticles have made them attractive as platforms for therapeutic and diagnostic agents. For example, nanoparticles are known for their high relative surface area compared to larger constructs, which enables the modular, multiplexed, and high-density functionalization of their surface (Fig. 6.13). Furthermore, the large size of nanoparticles compared to molecular entities also allows them to encapsulate small molecules. A wide variety of nanoparticles have been leveraged for biomedical applications, and their compositions can be broadly described as either organic or inorganic.

Nanoparticles themselves can act as tumor-targeting vectors by leveraging the *enhanced permeability and retention (EPR) effect* [38]. The rapid angiogenesis in solid tumors often leads to disorganized and flawed neovasculature and enhanced vascular permeability. These irregularities often allow nanoparticles or macromolecules to traverse through the defective blood vessels and accumulate in the tumors. Thus, unmodified nanoparticles of suitable sizes can passively target radionuclides to tumors. In addition, active targeting is also possible for enhanced tumor-seeking properties. In this case, targeting moieties are attached to the nanoparticles via surface modifications, as indicated in Fig. 6.13.
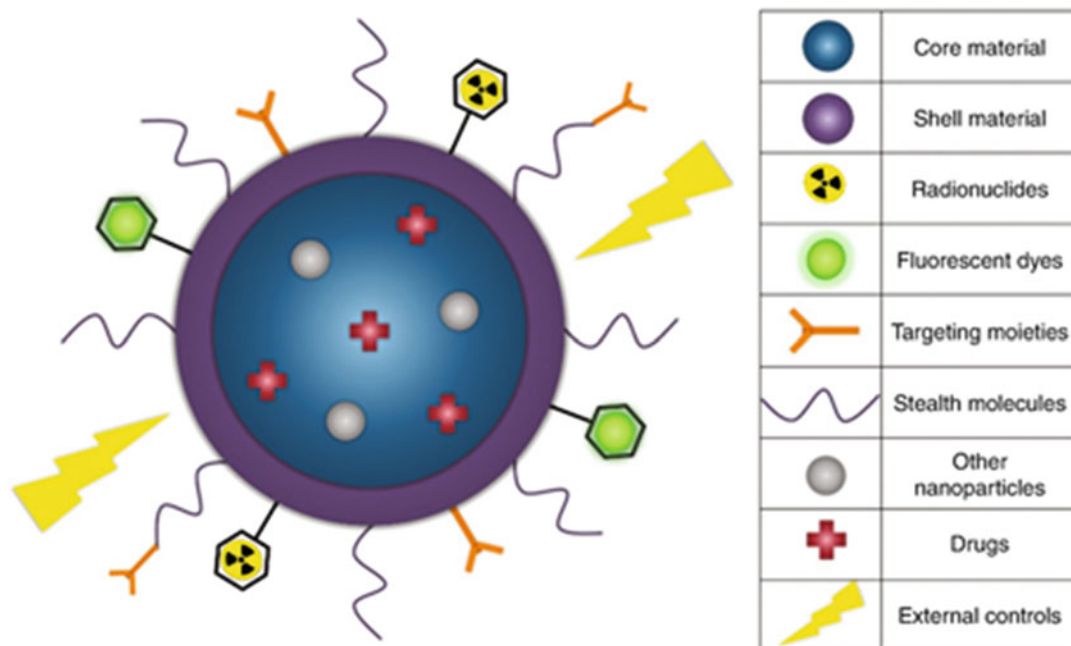
Fig. 6.13 Different cargoes can be appended to nanoparticles for therapeutic and diagnostic applications. (Reproduced from Ref. [37] with permission)

Another potential advantage of nanoparticles for RPT is their ability to handle and retain recoiling daughter nuclides. As detailed in Chap. 5, the conservation of momentum requires that daughter nuclides recoil with an opposite but equal momentum upon the emission of a particle. This phenomenon occurs with all radioactive emissions but is most important in the context of α-decay, in which the recoil energy exceeds that of chemical bonds by orders of magnitude. Thus, the decay of an α-emitting radiometal ruptures the metal–ligand bonds, freeing the daughter nuclide from the radiotherapeutic. In theory, the encapsulation of α-emitting radionuclides in nanoparticles could minimize the release of the recoiled daughter nuclides. This concept has been demonstrated with both inorganic and organic nanoparticles. For example, the incorporation of $^{225}Ac^{3+}$ into $LaPO_4$ nanoparticles led to the retention of ~50% of the ^{221}Fr and ^{213}Bi daughters within the nanoparticle [39]. Similarly, up to 69% of ^{221}Fr and 53% of ^{213}Bi were retained when $^{225}Ac^{3+}$ was encapsulated into polysomes

prepared from a poly(butadiene(1,2 addition)-b-ethylene oxide) block copolymer [40].

The radiolabeling of nanoparticles can be accomplished via two distinct pathways: *derivatization* and *incorporation* (Fig. 6.14) [41]. In derivatization, the nonradioactive nanoparticles are prepared first and then conjugated with the radiometal of interest. This approach is generally applied in conjunction with chelators. Typically, suitable chelators are attached to the nanoparticle surface in advance. For example, an analogue of DOTA (Fig. 6.6) was grafted onto *N,N,N*-trimethyl chitosan-coated magnetic nanoparticles, and the resulting construct was efficiently radiolabeled with $^{68}Ga^{3+}$ [42]. In polymeric nanoparticles, chelators can also be directly incorporated into the polymer backbone. In a recent study, a derivative of NOTA (Fig. 6.6) was attached to the building block of the polymeric chain, and the resulting nanoparticles were effectively radiolabeled with $^{68}Ga^{3+}$ [43].

The second nanoparticle radiolabeling strategy, *incorporation* or *intrinsic radiolabeling*
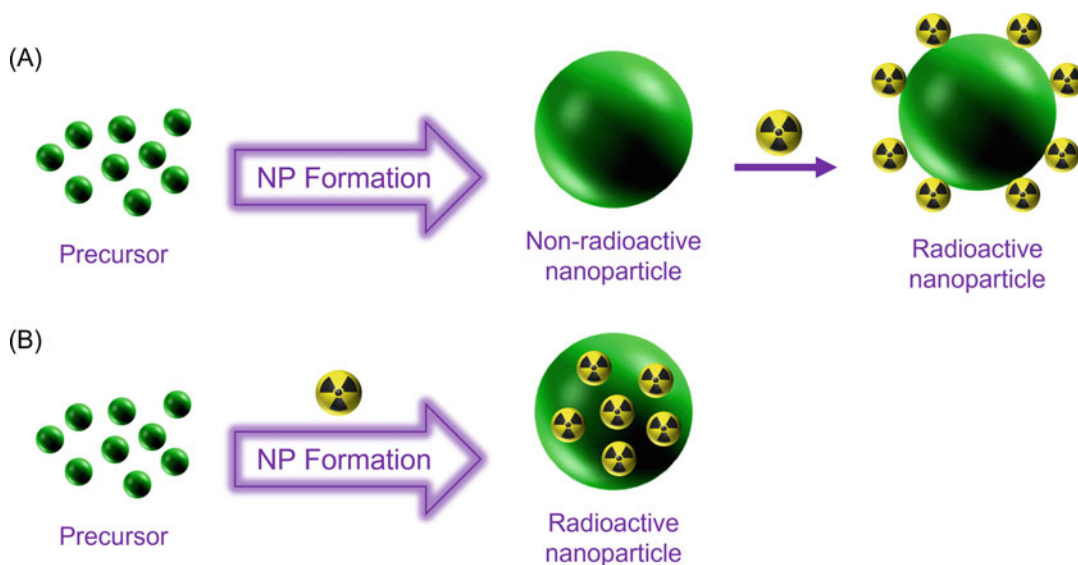
Fig. 6.14 Schematic illustration of the difference between the labeling of nanoparticles via (**a**) derivatization and (**b**) incorporation

[44], inserts the radiometal during the formation of the nanoparticle. An example of this approach was the inclusion of [198]Au during the formation of gold nanoparticles that were subsequently functionalized with epigallocatechin gallate (EGCg) to facilitate the targeting of prostate cancer tumors [45].

Despite the increasing research into the use of radiolabeled nanoparticles for RPT, the clinical translation of nanoparticulate radiopharmaceuticals remains at an early stage. One radiolabeled nanoparticle that has undergone clinical trials is [[188]Re]Re–BMEDA-liposome (Fig. 6.15) [46]. Its preparation employs the incorporation method. First, [[188]Re]ReO$_4^-$ is complexed by N,N-bis(2-mercaptoethyl)-N″,N″--diethylethylenediamine (BMEDA), and the radiometal complex is then incorporated into PEGylated liposomes. These liposomes leverage the EPR effect and have shown efficacy for the treatment of advanced solid ovarian tumors [47]. The clinical studies were initiated in 2014 but were terminated in 2020 due to the concerns surrounding the accumulation of radioactivity in the liver and spleen.

6.3   The Future

Harnessing metallic radiometals for RPT is a multidisciplinary endeavor that requires advances across several different fields. As new radiometals are identified as potential tools for RPT, new chemistry will be required to learn how to incorporate them into useful radiopharmaceuticals. Along these lines, the radiometals of unusual elements—including the actinides and transactinides—have driven and will continue to drive efforts to design novel ligands. Since the development and application of conventional chelators like DOTA and DTPA, extensive research has been dedicated to synthesizing and evaluating novel chelating agents. As highlighted in this chapter, these efforts have led to the development of chelators with greater radiolabeling efficiency and complex stability as well as unusual selectivity patterns (such as reverse and dual size selectivity). The use of nanoparticles for radiolabeling also provides intriguing opportunities. For example, the potential of nanoparticles to circumvent the

Fig. 6.15 Schematic depiction of [^{188}Re]Re– BMEDA-liposome

[^{188}Re]Re–BMEDA
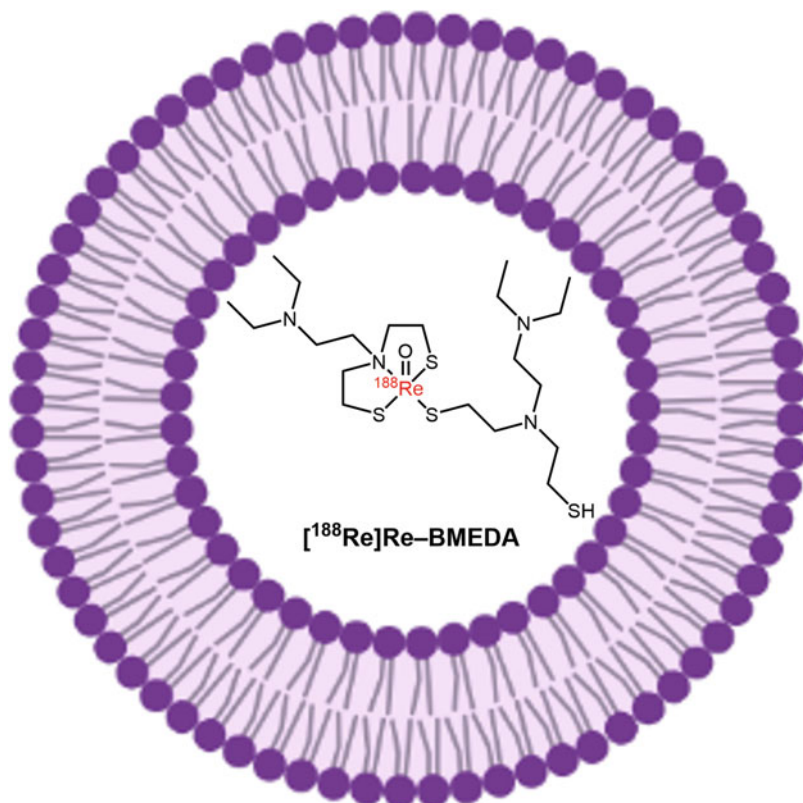
α recoil effect could facilitate the development of safer α-emitting agents for RPT. We also envision that advances in molecular and cellular biology will give rise to new targeting vectors, which will further enhance the selectivity, safety, and efficacy of radiopharmaceutical agents.

6.4 The Bottom Line

- A large number of metallic elements have radioisotopes that are relevant to RPT. These elements span the entirety of the periodic table and thus have distinct chemical properties. It is important to take these properties into account when designing novel radiometallated therapeutic agents.
- Different methods have been applied to leverage the radiometal ions for RPT. The radiometals can be administered as free metal salts or as components of larger radiopharmaceuticals based on small molecules, peptides, proteins, antibodies, or nanoparticles.

- It is often important to attach radiometals to targeting vectors to ensure the delivery of the former to target tissue in vivo. When building radiotherapeutics predicated on metal–ligand complexes, the ligand(s) must efficiently bind the radiometal and form a thermodynamically and kinetically stable complex.
- The successful transformation of a metallic radionuclide into a useful component of a radiotherapeutic requires a careful and lengthy design and assessment process. To this end, expertise in a variety of fields is needed.

References

1. Blower PJ. A nuclear chocolate box: the periodic table of nuclear medicine. Dalton Trans. 2015;44:4819–44. https://doi.org/10.1039/C4DT02846E.
2. Boros E, Packard AB. Radioactive transition metals for imaging and therapy. Chem Rev. 2019;119:870–901. https://doi.org/10.1021/acs.chemrev.8b00281.
3. Kostelnik TI, Orvig C. Radioactive main group and rare earth metals for imaging and therapy. Chem Rev.

2019;119:902–56. https://doi.org/10.1021/acs.chemrev.8b00294.

4. Poonia NS, Bajaj AV. Coordination chemistry of alkali and alkaline earth cations. Chem Rev. 1979;79:389–445. https://doi.org/10.1021/cr60321a002.

5. Shimoni-Livny L, Glusker JP, Bock CW. Lone pair functionality in divalent lead compounds. Inorg Chem. 1998;37:1853–67. https://doi.org/10.1021/ic970909r.

6. Seth SK, Bauzá A, Mahmoudi G, Stilinović V, López-Torres E, Zaragoza G, et al. On the importance of Pb···X (X = O, N, S, Br) tetrel bonding interactions in a series of tetra- and hexa-coordinated Pb(II) compounds. CrystEngComm. 2018;20:5033–44. https://doi.org/10.1039/C8CE00919H.

7. Figgis BN, Hitchman MA. Ligand field theory and its applications. New York: Wiley-VCH; 2000.

8. Shannon RD. Revised effective ionic radii and systematic studies of interatomic distances in halides and chalcogenides. Acta Crystallogr Sect A: Found Adv. 1976;32:751–67. https://doi.org/10.1107/S0567739476001551.

9. Seitz M, Oliver AG, Raymond KN. The lanthanide contraction revisited. J Am Chem Soc. 2007;129:11153–60. https://doi.org/10.1021/ja072750f.

10. Lewington VJ. Bone-seeking radionuclides for therapy. J Nucl Med. 2005;46:38S–47S.

11. Nightengale B, Brune M, Blizzard SP, Ashley-Johnson M, Slan S. Strontium chloride Sr 89 for treating pain from metastatic bone disease. Am J Health Syst Pharm. 1995;52:2189–95. https://doi.org/10.1093/ajhp/52.20.2189.

12. Kluetz PG, Pierce W, Maher VE, Zhang H, Tang S, Song P, et al. Radium Ra 223 dichloride injection: U.S. food and drug administration drug approval summary. Clin Cancer Res. 2014;20:9–14. https://doi.org/10.1158/1078-0432.CCR-13-2665.

13. da Silva Frausto JJR. The chelate effect redefined. J Chem Educ. 1983;60:390. https://doi.org/10.1021/ed060p390.

14. Martell AE, Hancock RD. Metal complexes in aqueous solutions. New York: Plenum Press; 1996.

15. Harris WR, Carrano CJ, Raymond KN. Coordination chemistry of microbial iron transport compounds. 16. Isolation, characterization, and formation constants of ferric aerobactin. J Am Chem Soc. 1979;101:2722–7. https://doi.org/10.1021/ja00504a038.

16. Anderson PM, Wiseman GA, Dispenzieri A, Arndt CAS, Hartmann LC, Smithson WA, et al. High-dose samarium-153 ethylene diamine tetramethylene phosphonate: low toxicity of skeletal irradiation in patients with osteosarcoma and bone metastases. J Clin Oncol. 2002;20:189–96. https://doi.org/10.1200/JCO.2002.20.1.189.

17. Wester H-J, Schottelius M. PSMA-targeted radiopharmaceuticals for imaging and therapy. Semin Nucl Med. 2019;49:302–12. https://doi.org/10.1053/j.semnuclmed.2019.02.008.

18. Sartor O, Herrmann K. Prostate cancer treatment: ^{177}Lu-PSMA-617 considerations, concepts, and limitations. J Nucl Med. 2022;63:823–9. https://doi.org/10.2967/jnumed.121.262413.

19. Hennrich U, Kopka K. Lutathera®: the first FDA- and EMA-approved radiopharmaceutical for peptide receptor radionuclide therapy. Pharmaceuticals. 2019;12:114. https://doi.org/10.3390/ph12030114.

20. Rogoza O, Megnis K, Kudrjavceva M, Gerina-Berzina A, Rovite V. Role of somatostatin signalling in neuroendocrine tumours. Int J Mol Sci. 2022;23:1447. https://doi.org/10.3390/ijms23031447.

21. Grillo-López AJ. Zevalin: the first radioimmunotherapy approved for the treatment of lymphoma. Expert Rev Anticancer Ther. 2002;2:485–93. https://doi.org/10.1586/14737140.2.5.485.

22. van Meerten T, Hagenbeek A. CD20-targeted therapy: the next generation of antibodies. Semin Hematol. 2010;47:199–210. https://doi.org/10.1053/j.seminhematol.2010.01.007.

23. Lindoy LF. What is different about macrocyclic ligand complexes? In: The chemistry of macrocyclic ligand complexes. Cambridge: Cambridge University Press; 1989. p. 1–20.

24. Hancock RD, Martell AE. The chelate, cryptate and macrocyclic effects. Comments Inorg Chem. 1988;6:237–84. https://doi.org/10.1080/02603598808072293.

25. Stasiuk GJ, Long NJ. The ubiquitous dota and its derivatives: the impact of 1,4,7,10-tetraazacyclododecane-1,4,7,10-tetraacetic acid on biomedical imaging. Chem Commun. 2013;49:2732–46. https://doi.org/10.1039/C3CC38507H.

26. Price EW, Orvig C. Matching chelators to radiometals for radiopharmaceuticals. Chem Soc Rev. 2014;43:260–90. https://doi.org/10.1039/C3CS60304K.

27. Wu C, Kobayashi H, Sun B, Yoo TM, Paik CH, Gansow OA, et al. Stereochemical influence on the stability of radio-metal complexes in vivo. synthesis and evaluation of the four stereoisomers of 2-(p-nitrobenzyl)-trans-CyDTPA. Bioorg Med Chem. 1997;5:1925–34. https://doi.org/10.1016/S0968-0896(97)00130-2.

28. Hu A, Wilson JJ. Advancing chelation strategies for large metal ions for nuclear medicine applications. Acc Chem Res. 2022;55:904–15. https://doi.org/10.1021/acs.accounts.2c00003.

29. Roca-Sabio A, Mato-Iglesias M, Esteban-Gómez D, Tóth É, de Blas A, Platas-Iglesias C, et al. Macrocyclic receptor exhibiting unprecedented selectivity for light lanthanides. J Am Chem Soc. 2009;131:3331–41. https://doi.org/10.1021/ja808534w.

30. Thiele NA, MacMillan SN, Wilson JJ. Rapid dissolution of baSO$_4$ by macropa, an 18-membered macrocycle with high affinity for Ba^{2+}. J Am Chem Soc. 2018;140:17071–8. https://doi.org/10.1021/jacs.8b08704.

31. Hu A, MacMillan SN, Wilson JJ. Macrocyclic ligands with an unprecedented size-selectivity pattern for the lanthanide ions. J Am Chem Soc. 2020;142:13500–6. https://doi.org/10.1021/jacs.0c05217.

32. Hu A, Aluicio-Sarduy E, Brown V, MacMillan SN, Becker KV, Barnhart TE, et al. Py-macrodipa: a janus chelator capable of binding medicinally relevant rare-earth radiometals of disparate sizes. J Am Chem Soc. 2021;143:10429–40. https://doi.org/10.1021/jacs.1c05339.

33. Nunn AD. New radiopharmaceuticals based on technetium. In: Schubiger PA, Westera G, editors. Progress in radiopharmacy. Dordrecht: Springer Science+Business Media; 1992. p. 55–65.

34. Bodnar EN, Dikiy MP, Medvedeva EP. Photonuclear production and antitumor effect of radioactive cisplatin (^{195m}Pt). J Radioanal Nucl Chem. 2015;305:133–8. https://doi.org/10.1007/s10967-015-4053-1.

35. Lepareur N, Lacœuille F, Bouvry C, Hindré F, Garcion E, Chérel M, et al. Rhenium-188 labeled radiopharmaceuticals: current clinical applications in oncology and promising perspectives. Front Med. 2019;6:132. https://doi.org/10.3389/fmed.2019.00132.

36. Blower PJ, Kettle AG, O'Doherty MJ, Coakley AJ, Knapp FF Jr. ^{99m}Tc(V)DMSA quantitatively predicts ^{188}Re(V)DMSA distribution in patients with prostate cancer metastatic to bone. Eur J Nucl Med. 2000;27:1405–9. https://doi.org/10.1007/s002590000307.

37. Kamkaew A, Ehlerding EB, Cai W. Nanoparticles as radiopharmaceutical vectors. In: Lewis JS, Windhorst AD, Zeglis BM, editors. Radiopharmaceutical chemistry. Cham: Springer Nature Switzerland AG; 2019. p. 181–203.

38. Fang J, Nakamura H, Maeda H. The EPR effect: unique features of tumor blood vessels for drug delivery, factors involved, and limitations and augmentation of the effect. Adv Drug Deliv Rev. 2011;63:136–51. https://doi.org/10.1016/j.addr.2010.04.009.

39. Woodward J, Kennel SJ, Stuckey A, Osborne D, Wall J, Rondinone AJ, et al. LaPO4 nanoparticles doped with actinium-225 that partially sequester daughter radionuclides. Bioconjug Chem. 2011;22:766–76. https://doi.org/10.1021/bc100574f.

40. Wang G, de Kruijff RM, Rol A, Thijssen L, Mendes E, Morgenstern A, et al. Retention studies of recoiling daughter nuclides of ^{225}Ac in polymer vesicles. Appl Radiat Isot. 2014;85:45–53. https://doi.org/10.1016/j.apradiso.2013.12.008.

41. Dai W, Zhang J, Wang Y, Jiao C, Song Z, Ma Y, et al. Radiolabeling of nanomaterials: advantages and challenges. Front Toxicol. 2021;3:753316. https://doi.org/10.3389/ftox.2021.753316.

42. Hajiramezanali M, Atyabi F, Mosayebnia M, Akhlaghi M, Geramifar P, Jalilian AR, et al. ^{68}Ga-radiolabeled bombesin-conjugated to trimethyl chitosan-coated superparamagnetic nanoparticles for molecular imaging: preparation, characterization and biological evaluation. Int J Nanomedicine. 2019;14:2591–605. https://doi.org/10.2147/IJN.S195223.

43. Körhegyi Z, Rózsa D, Hajdu I, Bodnár M, Kertész I, Kerekes K, et al. Synthesis of ^{68}Ga-labeled biopolymer-based nanoparticle imaging agents for positron-emission tomography. Anticancer Res. 2019;39:2415–27. https://doi.org/10.21873/anticanres.13359.

44. Goel S, Chen F, Ehlerding EB, Cai W. Intrinsically radiolabeled nanoparticles: an emerging paradigm. Small. 2014;10:3825–30. https://doi.org/10.1002/smll.201401048.

45. Ravi S, Nripen C, Ajit Z, Anandhi U, Kavita K, Kulkarni RR, et al. Laminin receptor specific therapeutic gold nanoparticles (^{198}AuNP-EGCg) show efficacy in treating prostate cancer. Proc Natl Acad Sci. 2012;109:12426–31. https://doi.org/10.1073/pnas.1121174109.

46. Anselmo AC, Mitragotri S. Nanoparticles in the clinic: an update post covid-19 vaccines. Bioeng Transl Med. 2021;6:e10246. https://doi.org/10.1002/btm2.10246.

47. Chang C-M, Lan K-L, Huang W-S, Lee Y-J, Lee T-W, Chang C-H, et al. ^{188}Re-liposome can induce mitochondrial autophagy and reverse drug resistance for ovarian cancer: from bench evidence to preliminary clinical proof-of-concept. Int J Mol Sci. 2017;18:903. https://doi.org/10.3390/ijms18050903.